

ρ -Meson Production and Decay in Proton-Nucleus Collisions*

A. Sibirtsev and W. Cassing

Institut für Theoretische Physik, Universität Giessen
D-35392 Giessen, Germany

June 16, 2021

PACS: 24.10.-i; 24.30.-v; 24.50.+g; 25.40.-h

Keywords: resonance model, meson exchange model, medium mass modification, pion production

Abstract

We analyze the production of ρ -mesons in $p + A$ reactions including both the production by proton-nucleon as well as pion-nucleon collisions within a coupled channel transport approach. The final state interactions of the ρ -meson with nucleons are evaluated from a resonance model which allows to extract elastic and inelastic cross sections. We include the latter final state interactions, the ρ -meson decay into two pions as well as the final pion-nucleon interactions within the transport approach. We find the invariant mass distribution of pion pairs to be sensitive to the ρ -meson properties in the nuclear medium. However, due to the strong final state interactions of pions only light targets like ^{12}C might be suited to extract a ρ -signal from the uncorrelated two pion background which carries information about the in-medium properties of the ρ -meson.

*Supported by Forschungszentrum Jülich

1 Introduction

The restoration of chiral symmetry at high baryon density or temperature nowadays is a question of primary interest. As suggested a long time ago the short lived ρ -meson is a primary candidate to study possible in-medium mass shifts or dispersion relations as e.g. predicted by Brown - Rho scaling [1] or QCD sum-rules [2]. Whereas the dileptonic decay of the ρ -meson appears as an ideal probe of the in-medium properties of the ρ -meson, the two pion hadronic decay in principle carries the same information provided that the decay products suffer only little rescattering.

At SPS energies the dilepton data of the CERES [3] and HELIOS-3 Collaborations [4] have indicated a possible mass shift of the ρ -meson following the analysis of Li, Ko and Brown [5] as well as Cassing et al. [6, 7, 8]. A recent summary of the situation has been given by Drees [9]. However, the approaches in [5] and [6] differ in the actual assumptions on the ρ -meson mass shift. In the model of Ref. [5] a dropping of the ρ -mass at normal nuclear matter density ρ_0 of about 30-35% is employed whereas in the transport study of Ref. [6, 7, 8] the ρ -mass drops only by about 18% at ρ_0 in line with the QCD sum-rule study of Hatsuda and Lee [2]. Such drastic in-medium effects should also be seen in proton-nucleus or pion-nucleus collisions [10, 11] via the electromagnetic decay of the ρ -meson or even the ω -meson in case of $\pi + A$ reactions [10].

In the present paper we explore the possibility if such medium effects of the ρ -meson might also be measured by two-pion invariant mass distributions in proton-nucleus reactions. Our study thus is organized as follows: In Section 2 we present the elementary ρ -meson production cross sections from nucleon-nucleon and pion-nucleon collisions and determine the elastic and inelastic cross sections of the ρ -mesons with nucleons from a resonance model. In Section 3 we discuss possible in-medium modifications of the ρ -meson as incorporated in the present simulations. In Section 4 we test our transport approach with respect to pion spectra in proton-nucleus reactions. Section 5 is devoted to the actual ρ and pion dynamics in $p + {}^{12}\text{C}$ reactions at 2 - 2.5 GeV as well as to the reconstruction of the ρ -mass distribution from two-pion invariant mass spectra, while Section 6 concludes our work with a summary and discussion of open problems.

2 Elementary cross sections

2.1 ρ -meson production

In a previous study we have investigated the production of vector mesons from proton-nucleus reactions from subthreshold energies to a few GeV employing empirical spectral functions [12]. It was found that at subthreshold energies the dominant contribution to ρ -meson production stems from secondary $\pi + N$ interactions while at energies above 2 GeV the primary proton-nucleon channel becomes more important. In the latter study the cross section for ρ -meson production from $\pi + N$ collisions was separated into two parts: i) an exclusive cross section related to binary processes ($\pi N \rightarrow \rho N$), which is dominant at energies close to the reaction threshold, and ii) the inclusive production of

ρ -mesons at higher energies which is dominated by phase space and can be described by the LUND string model [13].

The cross section for the exclusive reaction $\pi + N \rightarrow \rho + N$ can be obtained - in the limit of vanishing interference terms - via an incoherent summation over all baryonic resonances decaying into ρN channels [14, 15, 16] as

$$\sigma_{\pi N \rightarrow \rho N} = \frac{\pi}{2k^2} \sum_R (2I_R + 1) \frac{\Gamma_{\pi N} \Gamma_{\rho N}}{(\sqrt{s} - M_R)^2 + \Gamma_R^2/4}, \quad (1)$$

where M_R and Γ_R are the mass and total width of the baryonic resonance, while $\Gamma_{\pi N}$ and $\Gamma_{\rho N}$ are the partial width for the initial and final state, respectively. Here k is the pion momentum in the resonance frame of reference. We account for a momentum dependence of the resonance width as [14, 17]

$$\Gamma(k) = \Gamma_0 \left(\frac{k}{k_R} \right)^{2l+1} \left(\frac{k_R^2 + \delta^2}{k^2 + \delta^2} \right)^{l+1}, \quad (2)$$

where k_R is the momentum at $\sqrt{s} = M_R$, l is the minimal orbital angular momentum of the system and $\delta^2 = 0.1 \text{ GeV}^2/c^2$.

The properties of the baryonic resonances are available for resonances up to a mass of about 2 GeV [20]. In order to describe the exclusive $\pi + N \rightarrow \rho + N$ reaction at energies above $\sqrt{s} \simeq 2 \text{ GeV}$ we incorporate additionally two 'effective' resonances with masses of 2.4 and 3.3 GeV; all resonance properties adopted are listed in Table.1.

Table 1: Properties of baryonic resonances used in the calculations. Apart from the known resonances we have added the 'effective' resonances $E1$ and $E2$ to describe properly the exclusive production of ρ mesons in πN reactions.

Resonance	I_R	M_R (MeV)	Γ_R (MeV)	$\rightarrow N\pi$ (%)	$\rightarrow N\rho$ (%)
F_{15}	5/2	1680	125	60	5
D_{13}	3/2	1700	100	10	10
P_{11}	1/2	1710	110	15	20
P_{13}	3/2	1720	150	10	70
F_{17}	7/2	1990	260	20	5
D_{33}	3/2	1700	280	15	30
S_{31}	1/2	1900	150	10	45
F_{35}	5/2	1905	350	10	72
P_{31}	1/2	1910	250	25	37
$E1$	3/2	2400	1000	70	25
$E2$	5/2	3300	1000	60	8

The experimental data for the exclusive reaction $\pi^+ + p \rightarrow \rho^+ + p$ [18] are shown by full squares in Fig. 1a) as a function of $\sqrt{s} - \sqrt{s_0}$, with \sqrt{s} denoting the invariant energy of the colliding particles while the threshold energy is given by $\sqrt{s_0} = m_N + m_\rho$.

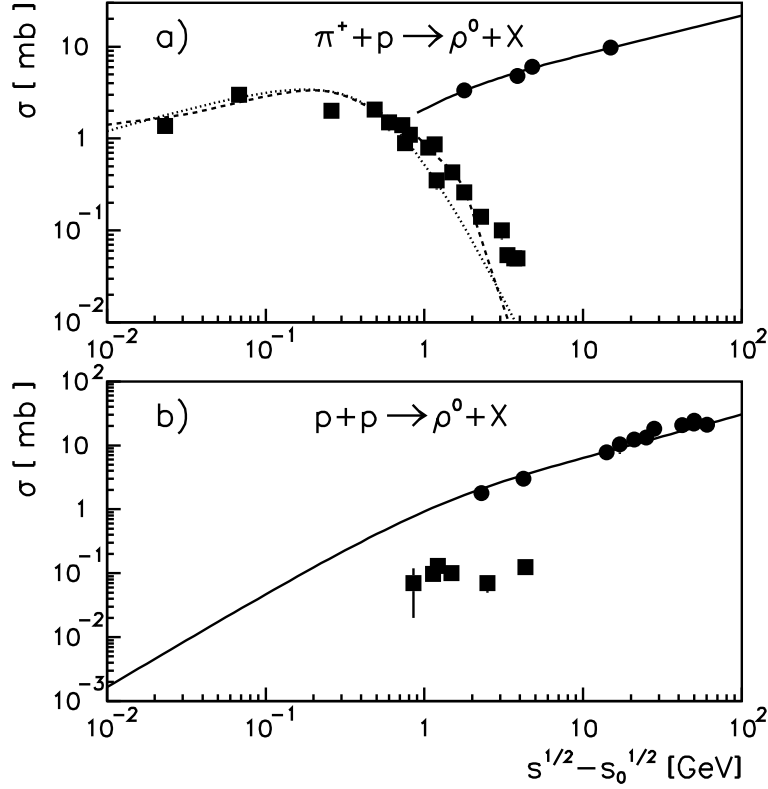


Figure 1: Cross sections for ρ -meson production in $\pi^+ + p$ (a) and $p + p$ interactions (b). The solid lines show the results from the LUND string model for the inclusive production cross section at higher energies, while the dashed line in (a) is calculated within the effective resonance model (1). The dotted line in (a) is the parametrization from [12]. The experimental data are taken from [18] and show the cross sections for the exclusive reaction $\pi^+ p \rightarrow \rho^+ p$ (full squares) (a) and $pp \rightarrow \rho^0 pp$ (full squares) (b) as well as for the inclusive reactions $\pi^+ p \rightarrow \rho^0 + X$ (full circles) (a) and $pp \rightarrow \rho^0 + X$ (full circles) (b).

The calculated cross section within the resonance model (1) is shown in Fig. 1a) by the dashed line. Note that for energies above $\sqrt{s} - \sqrt{s_0} \simeq 0.3$ GeV a reasonable reproduction of the experimental data is only possible due to an incorporation of the two 'effective' resonances E1 and E2 as given in Table 1. The dotted line in Fig. 1a) shows the parametrization from Ref. [12] for comparison and practically coincides with our present result from (1).

Since the available experimental data show no difference [19] between the reactions $\pi^- + p \rightarrow \rho^0 + n$, $\pi^- + p \rightarrow \rho^- + p$ and $\pi^+ + p \rightarrow \rho^+ + p$ we assume in the following that the cross sections are the same for π^+ , π^- and π^0 , for neutrons and protons as well as for ρ^+ , ρ^- and ρ^0 -mesons, respectively.

At low energies above threshold only the exclusive reactions discussed above are

energetically allowed. However, an additional production of pions, i.e. $\pi + N \rightarrow \rho + N + \pi$'s, is possible above $\sqrt{s} - \sqrt{s_0} \geq m_\pi$. Since there are not enough experimental data available for the inclusive ρ -meson production from $\pi + N$ collisions that allow to construct reliable parametrizations, we calculate the cross sections for the inclusive reactions within the Lund-String-Model (LSM) from [13]. The calculated results within the LSM can be fitted by

$$\sigma(\pi + p \rightarrow \rho + X) = 3.6 [mb] \times (x - 1)^{1.47} \times x^{-1.25}, \quad (3)$$

where $x = s/s_0$ and $s_0 = (m_N + m_\rho)^2$. Our fit to the LSM results is shown by the solid line in Fig. 1a) and reasonably well reproduces the available inclusive data on ρ -meson production (full circles) at higher energies.

For the ρ -meson production from nucleon-nucleon collisions we use the parametrization obtained within the LSM as [12]

$$\sigma(p + p \rightarrow \rho + X) = 2.2 [mb] \times (x - 1)^{1.47} \times x^{-1.1} \quad (4)$$

with $x = s/s_0$ and $s_0 = (2m_N + m_\rho)^2$ for the nucleon-nucleon channels. The fit (4) to the LSM results is shown by the solid line in Fig. 1b) in comparison to the experimental data for the inclusive production of ρ -mesons (full circles) from [18]. For comparison we additionally show the cross section for the exclusive reaction $p + p \rightarrow p + p + \rho^0$ (full triangles) from [18], which about 1 GeV above threshold is already small compared to the inclusive cross section. Furthermore, we assume that the cross sections are isospin independent for all possible nucleon-nucleon channels allowed by charge conservation.

Fig.1 clearly demonstrates that the cross section for ρ -meson production from pion induced reactions is significantly larger than that from nucleon-nucleon collisions at the same available energy above the threshold. As a consequence the pion induced channels dominate for ρ meson production also in $p + A$ reactions close to the absolute threshold energies as shown in Ref. [12].

2.2 ρN interactions

The absorption of ρ -mesons in the nucleus due to the reactions $\rho + N \rightarrow m\pi + N$ with $m \geq 1$ substantially attenuates the cross section and spectrum of ρ -mesons in $p + A$ collisions. To account for the ρ -meson interaction in finite nuclei we need the $\rho + N$ cross section at nuclear densities from 0 to $\rho_0 \approx 0.17 fm^{-3}$. Since detailed Brueckner calculations for these reactions in the medium are not available we assume that the in-medium cross sections are approximately the same as those in the vacuum. In the latter case the total and elastic ρN cross sections can be calculated within the resonance model as

$$\sigma_{\rho N} = \frac{\pi}{6k^2} \sum_R (2I_R + 1) \frac{\Gamma_{\rho N} \Gamma_{out}}{(\sqrt{s} - M_R)^2 + \Gamma_R^2/4}, \quad (5)$$

where M_R , Γ_R and $\Gamma_{\rho N}$ denote the mass, total and partial width ($R \rightarrow \rho N$) of the baryonic resonances, respectively. In Eq. (5) k now is the momentum of the ρ -meson in the resonance frame. The summation is performed again over all the baryonic

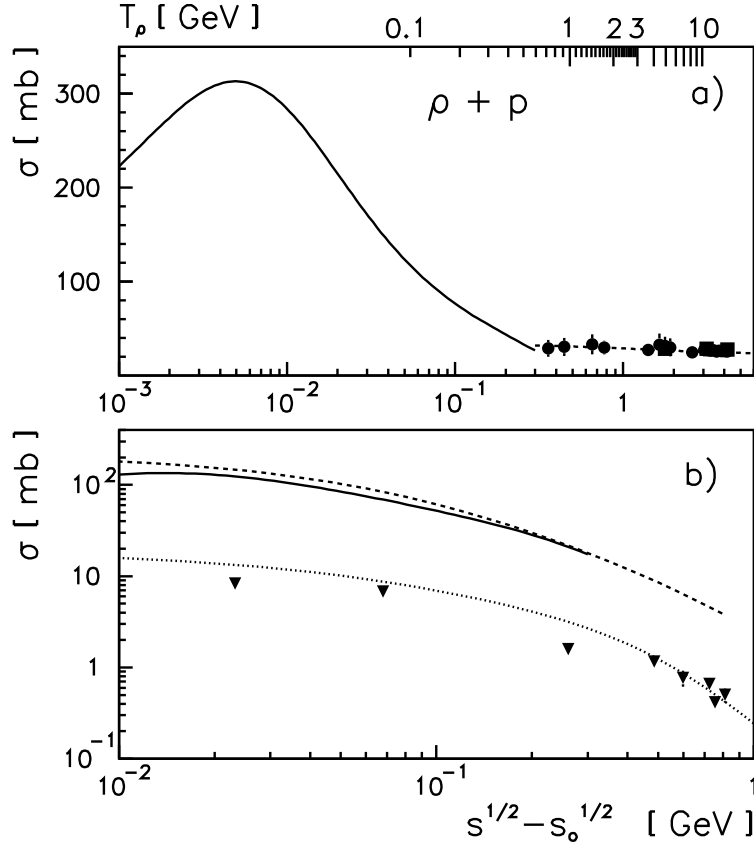


Figure 2: Cross sections for $\rho + p$ interactions: a) shows the total cross section; the solid line is the calculation with the resonance model (5), while the dashed line indicates the quark model relation (6). The solid circles show the experimental data extracted from vector dominance (11); the squares are the data from [28]. b) The solid line shows the elastic cross section from the resonance model (5), while the dashed line results from the σ -exchange calculations (7). The dotted line and the triangles indicate the cross section for the reaction $\rho + N \rightarrow \pi + N$ obtained by detailed balance (12,13).

resonances listed in Table.1 thus neglecting the interference between the resonances. The $\rho + N$ total cross section is calculated with $\Gamma_{out} = \Gamma_R$ while the elastic cross section is evaluated with $\Gamma_{out} = \Gamma_{\rho N}$.

The result of our calculations for the $\rho + N$ total cross section is shown in Fig.2a) (solid line), while the elastic cross section is shown in Fig.2b) (solid line); both are displayed up to $\sqrt{s} - m_N - m_\rho \simeq 0.3$ GeV, only, because we do not include in our calculation the heavier baryonic resonances E1 and E2 due to possibly improper branching ratios. In view of the neglect of interference terms and the limited energy range considered our calculations should only be considered as an estimate that will have to be improved in future. We note, however, that a momentum dependent width according to Eq. (2) compared to a fixed average width does not change these cross sections in Fig. 2 sizeably.

Following the quark model relations one can express the cross section for the $\rho + N$ interaction at high energies in terms of pion-nucleon cross sections as

$$\sigma_{\rho^0 N} = \frac{1}{2} (\sigma_{\pi^- N} + \sigma_{\pi^+ N}). \quad (6)$$

The total $\rho + N$ cross section according to Eq.(6) is shown in Fig.2a) by the dashed line. For the πN cross sections entering here we have used a Regge fit to the experimental data from [20]. Note, that there is a reasonable agreement between the results from the resonance model and the quark model in the overlapping energy region.

The calculation of the $\rho + N \rightarrow \rho + N$ elastic scattering in an effective meson-exchange model may be restricted to a diagram with the σ -exchange [21]. In the t -channel the elastic cross section then can be expressed as

$$\sigma_{\rho N \rightarrow \rho N} = \frac{1}{8\pi} \frac{m_N^2}{4s} \int_{-1}^1 dx \bar{M}(s, x), \quad (7)$$

where s is the square of the total center-of-mass energy, m_N is the nucleon mass and the isospin averaged squared amplitude is given by [21, 22]

$$\bar{M}(s, x) = 4 \frac{g_{\sigma\rho\rho}^2 g_{\sigma NN}^2}{m_\rho^2} \left(1 - \frac{q^2}{4m_N^2}\right) \left(\frac{1}{q^2 - m_\sigma^2}\right)^2 \left(m_\rho^4 - \frac{m_\rho^2 q^2}{3} + \frac{q^4}{24}\right) F_{\sigma NN}^2 F_{\sigma\rho\rho}^2 \quad (8)$$

where

$$q^2 = \frac{[s - (m_N + m_\rho)^2][s - (m_N - m_\rho)^2]}{2s} (x - 1). \quad (9)$$

In Eq.(8) we use the monopole form factors

$$F_{\sigma NN} = \frac{\Lambda_1^2 - m_\sigma^2}{\Lambda_1^2 + q^2}, \quad F_{\sigma\rho\rho} = \frac{\Lambda_2^2 - m_\sigma^2}{\Lambda_2^2 + q^2}. \quad (10)$$

The cut-off parameters $\Lambda_1 = 0.9$ GeV and $\Lambda_2 = 1.0$ GeV as well as the constant $g_{\sigma\rho\rho}^2/4\pi = 14.8$ were taken from the recent analysis of Friman and Soyeur [23] on ρ -meson photoproduction off nucleons, while the coupling constant $g_{\sigma NN}^2/4\pi = 8$ and $m_\sigma = 550$ MeV were taken from the Bonn potential [24]. The elastic cross section calculated within the σ -exchange model is shown in Fig.2b) by the dashed line and reasonably agrees with that from the resonance model (solid line). Though the actual magnitude of this cross might change by about 30% in a more sophisticated analysis, it becomes clear that $\rho - N$ rescattering will be very important for the final ρ -meson spectra.

Furthermore, in a vector dominance model the photoproduction of a ρ -meson is related to the $\rho + N$ cross section as

$$\sigma_{\rho p}^2 = \frac{\gamma_\rho^2}{4\pi} \frac{64\pi}{\alpha} \left. \frac{d\sigma_{\gamma p \rightarrow \rho p}}{dt} \right|_{t=0} \quad (11)$$

where α is the fine-structure constant and the coupling constant $\gamma_\rho^2/4\pi = 0.61$ according to Ref.[25]. The solid circles in Fig.2a) show the total $\rho + p$ cross section calculated from the experimental forward ρ -photoproduction amplitudes from [25, 26, 27].

Furthermore, the squares in Fig.2a) show the $\rho + N$ cross section extracted from ρ -photoproduction on the deuteron ($\gamma + d \rightarrow \rho^0 + d$) independently of the vector dominance model [28].

The cross section for the $\rho + N \rightarrow \pi + N$ reaction channel may be obtained exploiting detailed balance as

$$\sigma_{\rho^+ p \rightarrow \pi^+ p} = \frac{1}{3} \frac{q_\pi^2}{q_\rho^2} \sigma_{\pi^+ p \rightarrow \rho^+ p} \quad (12)$$

and is shown by triangles in Fig.2b) using the experimental cross section of the inverse reaction from Ref. [18].

Note that Eq.(12) is only valid in case of stable particles. For a broad resonance as the ρ -meson it is easy to show [29] that

$$\sigma_{\rho^+ p \rightarrow \pi^+ p} = \frac{m_\rho}{6\pi} \frac{q_\pi^2}{q_\rho} \sigma_{\pi^+ p \rightarrow \rho^+ p} \left(\int_{2m_\pi}^{\sqrt{s}-m_N} dW W q_f \frac{\Gamma_\rho}{(W - m_\rho)^2 + \Gamma_\rho^2/4} \right)^{-1}, \quad (13)$$

where q_f is given as

$$q_f^2 = \frac{[s - (m_N + W)^2][s - (m_N - W)^2]}{4s}, \quad (14)$$

and m_ρ , Γ_ρ are the mass and width of the ρ -meson, respectively. The cross section for the reaction $\sigma_{\rho^+ p \rightarrow \pi^+ p}$ calculated by Eq.(13) within the prescription (1) for $\sigma_{\pi^+ p \rightarrow \rho^+ p}$ is shown in Fig.2b by the dotted line and differs only slightly from the prescription (12).

Note, that the results obtained from quite different approaches are in reasonable agreement with each other. At low energies $T_\rho \leq 200$ MeV the contribution from the inelastic reaction channels to the total cross section are dominant and much larger than the elastic cross section. Starting from a ρ kinetic energy of about 300 MeV the total cross section then stays constant at roughly 30 mb. Following the quark model the inelastic reaction channels to the total cross section are dominant here, too.

3 In-medium modifications of the ρ -meson

In the literature there are several approaches on the in-medium modifications of the ρ -meson. Without going into a detailed discussion we simply adopt two different models to explore the possibility if such modifications can be observed in the two-pion decay channel.

Following the results of Hatsuda [30] obtained from QCD sum-rules the in-medium mass m^* of the ρ -meson can be approximated as

$$m^* = m_B (1 - \alpha \rho_N / \rho_0) \quad (15)$$

where $\alpha = [0.16 \pm 0.06]$, $m_B = 0.7699$ GeV is the bare mass and ρ_N is the actual nuclear density, while $\rho_0 = 0.17 \text{ fm}^{-3}$.

Recently, the ρ -meson mass in finite nuclei was calculated by Saito, Tsushima and Thomas [31] within the quark-meson coupling model. The ratio m^*/m_B from [31, 32] for ^{12}C is shown in Fig.3 by the solid line as a function of the radial distance r . The

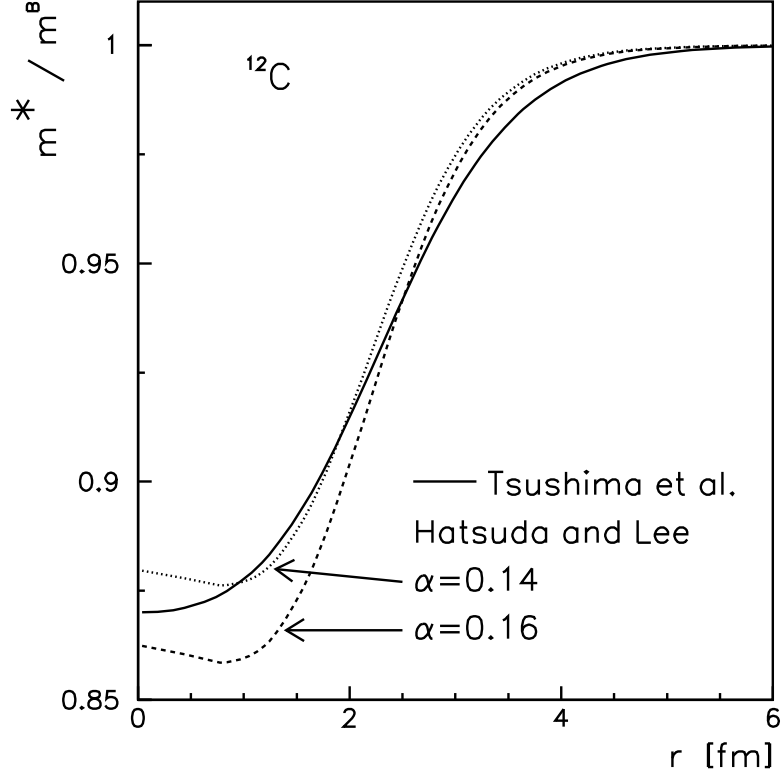


Figure 3: The ratio of the in-medium to the bare ρ -meson mass in a ^{12}C -target as a function of the distance r from the center of the nucleus. The solid line shows the numerical results from [31, 32], the dashed line is our result employing the linear parametrization (15) in a local density approximation for a parameter $\alpha = 0.16$ in Eq. (15) while the dotted line is obtained for $\alpha = 0.14$.

dashed line in Fig.3 illustrates the density dependence of the ρ -meson mass according to (15) for $\alpha = 0.16$ using the ^{12}C density distribution from [31, 32]. The dotted line is obtained for $\alpha = 0.14$, respectively. Note that the local density approximation works quite well in comparison to the calculations from Ref. [31, 32]. Indeed, the actual numerical results in [31, 32] show only a weak deviation from the linear parametrization [2, 33, 34] for a fixed nuclear density. In view of the uncertainty in the parameter α it thus appears justified to adopt the local density approximation further on. Accordingly, in the following calculations we will use the scaling (15) while keeping the width of the in-medium ρ -meson equal to the free one.

Furthermore, according to the hadronic model calculations of Klingl and Weise [35, 36] or Rapp, Chanfray and Wambach [37, 38] or Friman and Pirner [39] both the mass and the width of the ρ -meson are modified in nuclear matter. In our present study we use the results from [35, 36]. Actually, for the $\rho \rightarrow \pi\pi$ decay mode we need the general spectral function $A_R = dM_R/dM_{\pi\pi}$, i. e. the distribution of the resonance mass M_R with respect to the invariant mass of the two pions $M_{\pi\pi}$. The latter is related to the quantity $R^{I=1}$ from [35] as

$$A_R = \left(\frac{g_\rho}{m_B^2} \right)^2 \frac{s^{3/2}}{6\pi^2} \times R^{I=1}, \quad (16)$$

where $g_\rho = 6.05$ is the strong coupling constant, m_B the free ρ -meson mass and \sqrt{s} the invariant mass of the two pions. The solid line in Fig.4 shows the spectral function (16) of the ρ -meson at density $\rho_N = \rho_0$ calculated with $R^{I=1}$ from Ref. [40].

For numerical purposes we have parameterized (16) at invariant energies above $2m_\pi$ in the form

$$A_R = \frac{\Gamma_\rho}{(\sqrt{s} - m^*)^2 + \Gamma_\rho^2} a s^2 \quad (17)$$

with the parameters

$$\begin{aligned} \Gamma_\rho &= 2\Gamma_0 \\ m^* &= m_B (1 - 0.34\rho_N/\rho_0) \\ a &= 0.5 + 0.5\rho_N/\rho_0, \end{aligned} \quad (18)$$

$\Gamma_0 = 151$ MeV and m_B being the bare mass of the ρ -meson. The fit (17) is shown in Fig.4 by the full dots and reasonably reproduces the spectral function from Ref. [35, 40] at densities $\rho_0/2 \leq \rho_N \leq \rho_0$.

The dashed line in Fig.4 represents the ρ -meson spectral function in free space as

$$A_R = \frac{1}{2\pi} \frac{\Gamma_\rho}{(\sqrt{s} - m_\rho)^2 + \Gamma_\rho^2/4} \quad (19)$$

with $m_\rho = m_B$ while Γ_ρ is the momentum dependent ρ -meson width (2), respectively. Furthermore, the dotted line in Fig.4 shows the spectral function (19) with the free ρ -meson width and an average in-medium mass $m_\rho = m^*$ from Eq. (15) for $\alpha=0.16$.

In the following calculations we will use the different spectral functions in Fig.4 for a study of the ρ -meson production in $p + A$ collisions accounting for the in-medium modifications as discussed above.

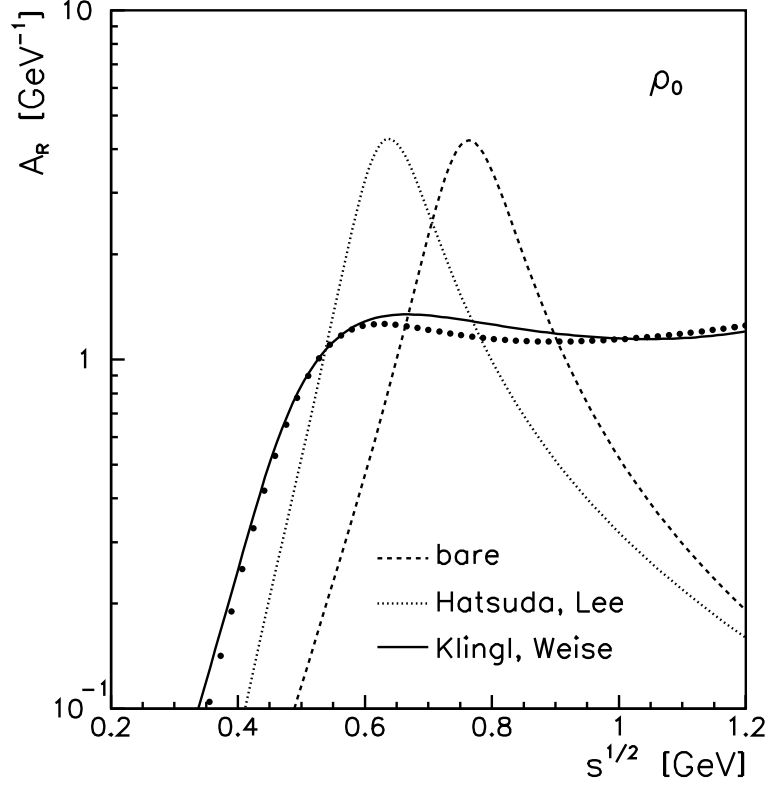


Figure 4: The spectral function of the ρ -meson from Klingl and Weise [35, 40] at normal nuclear matter density ρ_0 (solid line) in comparison with the spectral function in free space (dashed line); the dotted line displays the ρ -meson mass distribution according to Hatsuda and Lee [2] at ρ_0 for $\alpha = 0.16$ employing the free width of the ρ meson. The full dots show our parametrization (17) for the spectral function from Refs. [35, 40].

4 Background from uncorrelated pions

A proper calculation of the pion spectra from $p + A$ collisions is especially important for the study of ρ -meson production via the two pion decay mode ($\rho \rightarrow \pi\pi$), because multiple pion production from the reactions $p + A \rightarrow m\pi + X$ with $m \geq 2$, which are not associated with ρ -meson decays, substantially contribute to the invariant mass spectrum of two pions and have to be subtracted.

We use the coupled channel transport model [41] for the description of $p + A$ reactions that allows to account for the final state interactions of all hadrons and especially for those of the pions from the $\rho \rightarrow \pi\pi$ decay in the medium. The transport approach [41] is known to describe experimental data on pion production in a wide range of bombarding energies [41, 42]. Here, we briefly present a comparison with the experimental data available in the energy region of interest. Since the semiclassical transport approach [41] involves a local density approximation explicitly, this also serves as a test for the underlying assumptions of the dynamical model itself.

Fig.5 shows the spectrum of π^+ -mesons produced in $p + {}^{12}\text{C}$ collisions at 2.1 GeV at the pion emission angle of 2.5° in the laboratory. The data (full dots) from Ref. [43] are shown as a function of the Feynman variable $x_F = p_l^*/p_{max}^*$, where p_l^* is the longitudinal momentum of the pion in the center-of-mass system of the incident proton and nucleon at rest while p_{max}^* is defined as

$$p_{max}^* = \frac{([s - (m_N + m_\pi)^2][s - (m_N - m_\pi)^2])^{1/2}}{2\sqrt{s}}. \quad (20)$$

The solid line shows the scaling behaviour of the cross section from [44], which describes $p + A$ reactions from a bombarding energy of 1 GeV up to very high energies. The histogram represents our calculations within the transport approach and shows a good agreement with the experimental results.

Fig.6 shows the invariant cross section for π^+ -meson production from $p + {}^{12}\text{C}$ collisions at 2.5 GeV at an emission angle of 40° in the laboratory. The experimental data from the KaoS Collaboration [45] are shown by the full dots while the transport calculations are presented in terms of the histogram. We slightly overestimate the pion spectrum at high momenta and underestimate for $p_\pi \approx 0.5$ GeV/c. These deviations are basically due to the local density approximation employed in the transport model which is more uncertain in the surface of a light nucleus such as ${}^{12}\text{C}$. Though keeping in mind these minor deviations we conclude that the pion production and the proton-nucleus dynamics are described quite well within the transport approach such that we now can proceed with the ρ -meson and two-pion dynamics.

Due to the different kinematics for the production of multipion states and ρ -mesons from $p + A$ collisions the distribution of pion pairs in momentum space should be much broader; thus kinematical cuts could be used in order to enrich the contribution from ρ -meson decays. In this respect we show in Fig.7a the distribution in longitudinal and transverse momentum of pion pairs from $p + {}^{12}\text{C}$ collisions at 2.5 GeV, that do not stem from ρ -decays; Fig. 7b displays the corresponding momentum distribution of pion pairs from ρ -decays, respectively. As expected, the phase space of pion pairs from ρ -meson decay is substantially smaller than that for the uncorrelated pions. Using the

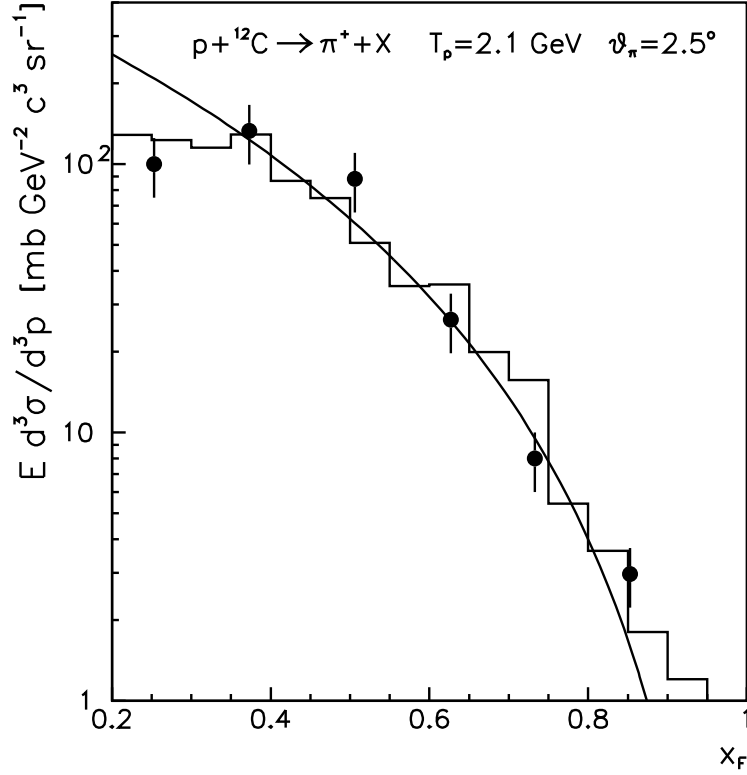


Figure 5: Invariant cross section for π^+ -meson production from $p + {}^{12}\text{C}$ collisions at 2.1 GeV at an emission angle of 2.5° in the laboratory as a function of the Feynman variable x_F . The full dots show the experimental data from [43]; the solid line is the scaling from [44] while the histogram shows our result calculated within the transport approach.

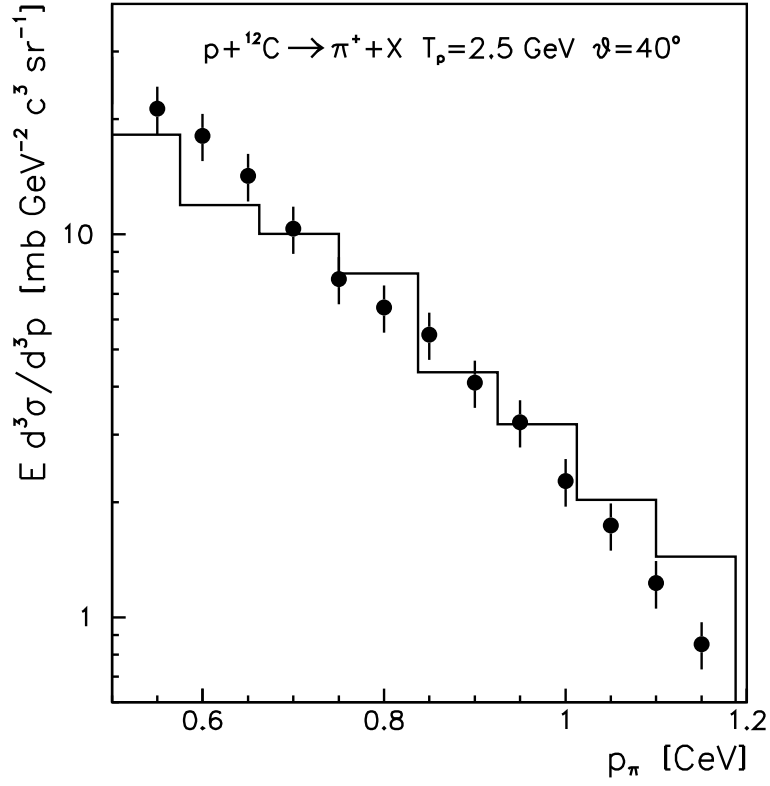


Figure 6: The invariant cross section for π^+ -production from $p + {}^{12}\text{C}$ collisions at 2.5 GeV at the pion emission angle of 40° in the laboratory. The experimental data [45] are shown by full dots while the histogram represents the result from the transport calculations.

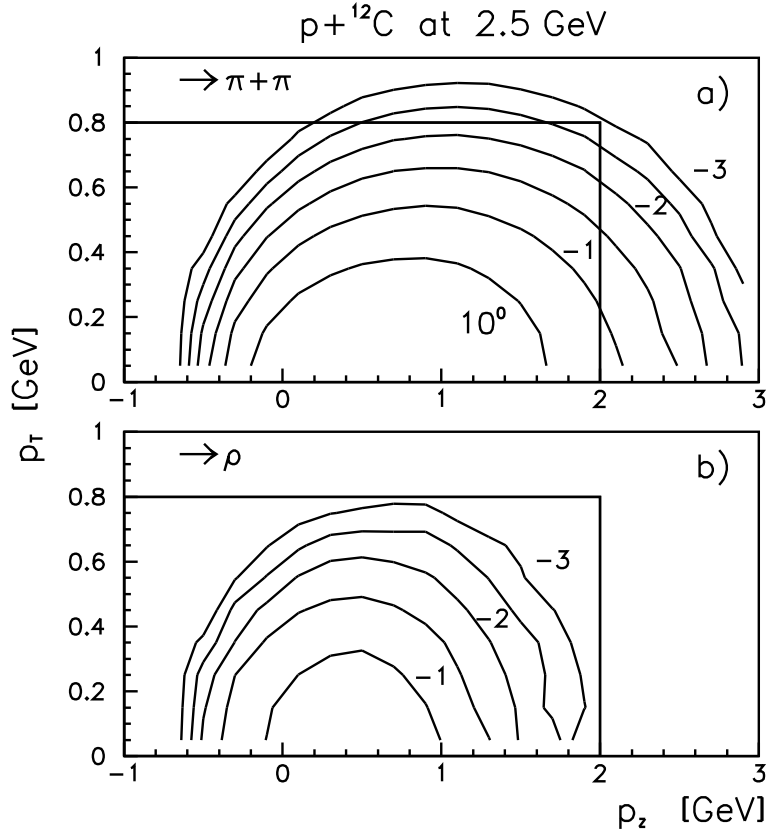


Figure 7: The longitudinal and transverse momentum distribution of pion pairs from $p + {}^{12}\text{C}$ collisions at 2.5 GeV; a) shows the results calculated for uncorrelated pion pairs while b) is for the pion pairs from ρ -decay. The rectangles indicate the cuts used in our analysis.

kinematical cuts as shown in Fig.7 ($p_z \leq 2$ GeV/c, $p_T \leq 0.8$ GeV/c) one can slightly enhance the ρ -meson signal in comparison to the background. In the following analysis we thus will always adopt the kinematical cuts $p_z \leq 2$ GeV/c and $p_T \leq 0.8$ GeV/c.

5 ρ -meson production from $p + A$ collisions.

The inclusive production of ρ -mesons for $p + {}^{12}\text{C}$ reactions has been calculated in Ref. [12] on the basis of empirical spectral functions for energies from the absolute threshold up to a few GeV. Since in this work we consider bombarding energies above 2 GeV the semiclassical transport approach employed should yield similar inclusive production cross sections when employing the same cross sections for the pN and πN production channels, respectively, and discarding any final state interactions of the ρ -mesons. In fact, by comparing the inclusive ρ^0 production cross sections in this limit from our transport approach with those from [12] for bombarding energies of 2 - 3 GeV (cf. Table 2) we find that both models differ only by about 20 %. The latter

deviations between the two approaches are due to the local density approximation and the on-shell assumption in the transport model. Since these differences are lower than the uncertainty in the elementary production cross sections we can use the coupled channel transport approach quite confidently for the following analysis, however, can include additionally all final state interactions of the ρ -mesons as well as for the pions which are more important in view of their large cross sections with nucleons.

Table 2: Comparison of the inclusive ρ^0 -production cross section in mb for $p + {}^{12}\text{C}$ reactions within the spectral function approach (SFA) [12] and our coupled channel transport approach (CBUU). For this comparison all final state interactions of the ρ -mesons have been discarded.

T (GeV)	SFA	CBUU
2.0	0.36	0.43
2.5	1.2	1.5
3.0	2.6	2.9

5.1 ρ -meson dynamics

We first investigate the 'clean' ρ^0 -meson production from $p + A$ collisions by neglecting the background from uncorrelated two pion pairs. The spectra of $\pi^+\pi^-$ pairs are shown in Fig.8 for $p + {}^{12}\text{C}$ and $p + {}^{208}\text{Pb}$ at a bombarding energy of 2.5 GeV as a function of their invariant mass. The calculations are performed for a bare ρ -meson spectral function (Fig.8a) and with an in-medium modification of the ρ -meson (Fig.8b) according to Eq.(15) for $\alpha = 0.16$. Note that the spectra for $p + {}^{12}\text{C}$ are displayed by hatched histograms and are scaled by a factor of 10 in order to compare the results for the light and the heavy target more directly.

The low energy part of the invariant mass distribution reflects the pion pairs from ρ -decays inside the nucleus that have suffered strong final state interactions. Obviously, such events are dominating for the heavy nucleus ${}^{208}\text{Pb}$. Even without medium modifications the ρ -resonance is practically melted and the mass distribution is close to a thermalized spectrum. For ${}^{12}\text{C}$ the rescattering of pions from ρ -decays is significantly reduced and a 'bare' ρ -meson signal or an in-medium ρ -meson signal can still be identified. In Fig.8c) we additionally show the calculated results for the invariant mass distribution of the pions from ρ decay for a ${}^{12}\text{C}$ target employing the parameters $\alpha = 0.16$ and 0.14, respectively, as in Fig. 3. The direct comparison demonstrates the relative sensitivity to the parameter α in the dropping mass scheme of Eq. (15); furthermore, it also demonstrates the relative uncertainty arising from the local density approximation in the transport approach since in view of Fig. 3 this uncertainty can be simulated by a corresponding change of the α parameter.

This initial study shows that the pion mode has substantial disadvantages compared to the dileptonic ρ -meson decay not only for the investigation of the in-medium

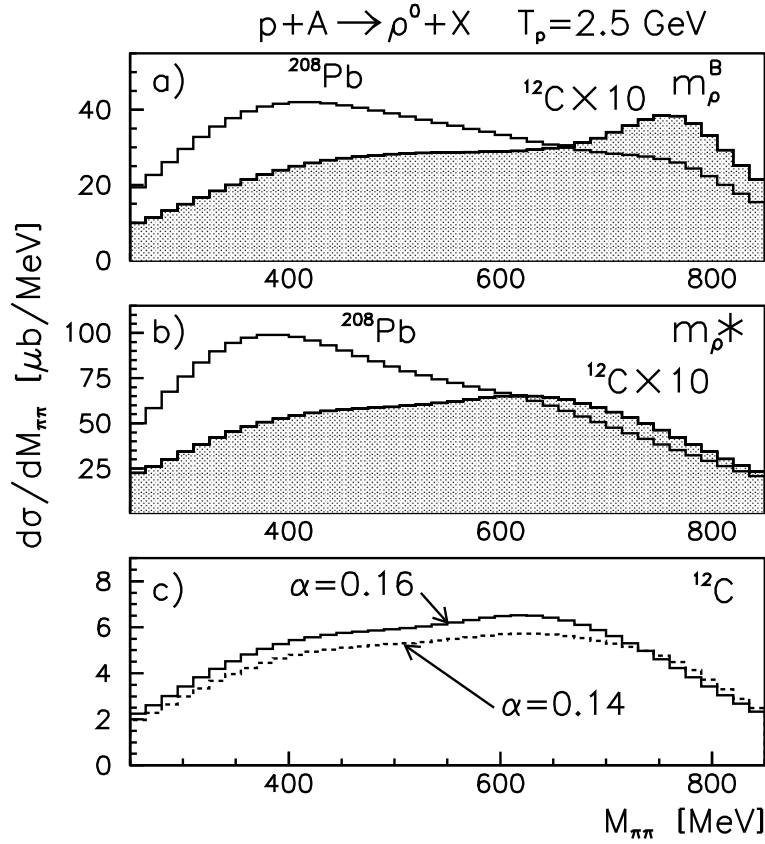


Figure 8: The invariant mass distribution of pion pairs from ρ -decays for $p + ^{12}\text{C}$ (hatched histogram) and $p + ^{208}\text{Pb}$ collisions at 2.5 GeV calculated with the bare (a) and in-medium (b) spectral function of the ρ -meson according to Eq. (15) for $\alpha = 0.16$; c) shows the calculated result in the dropping mass scenario for $\alpha = 0.16$ (solid histogram) and $\alpha = 0.14$ (dashed histogram), respectively. The spectra for ^{12}C are scaled by a factor of 10 in a) and b).

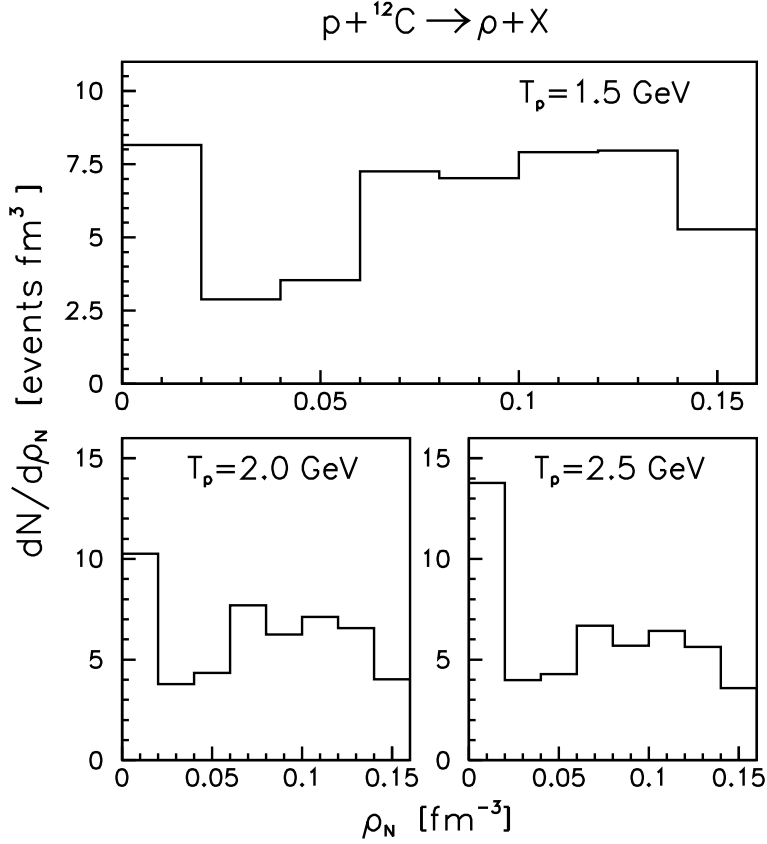


Figure 9: The distribution of the ρ -decay rate as a function of the nuclear density for $p + {}^{12}\text{C}$ collisions at bombarding energies of 1.5, 2.0 and 2.5 GeV.

properties of the ρ -meson but also for a conventional analysis of $p + A \rightarrow \rho + X$ reactions that rely on the reconstruction of the ρ -meson via two pion invariant mass distributions. The lightest target nuclei, however, may be used if the invariant mass spectrum is measured with a sufficiently high accuracy.

Of fundamental interest for the ρ -meson dynamics - relevant for in-medium modifications - is the distribution of the decay rate as a function of the nuclear density. Obviously, this distribution depends on the beam energy as well as on the size of the target and should be properly calculated within the transport approach. In this respect we display in Fig.9 the number of ρ -mesons decaying at the nuclear density ρ_N for $p + {}^{12}\text{C}$ collisions at bombarding energies of 1.5, 2.0 and 2.5 GeV. All distributions are normalized to 1 in order to illustrate the relative variation with the beam energy.

Note that events with densities $\rho_N \leq 0.05 \text{ fm}^{-3}$ can be associated with a ρ -meson decay at the periphery of the target or in the vacuum and carry no information about the medium effects. With increasing bombarding energy the nucleus becomes more transparent for the propagation of ρ -mesons due to lower total ρN cross sections and due to the fact that more ρ -mesons decay in the vacuum. Thus low energy collisions are more suitable to study the medium modification of ρ -meson properties, however,

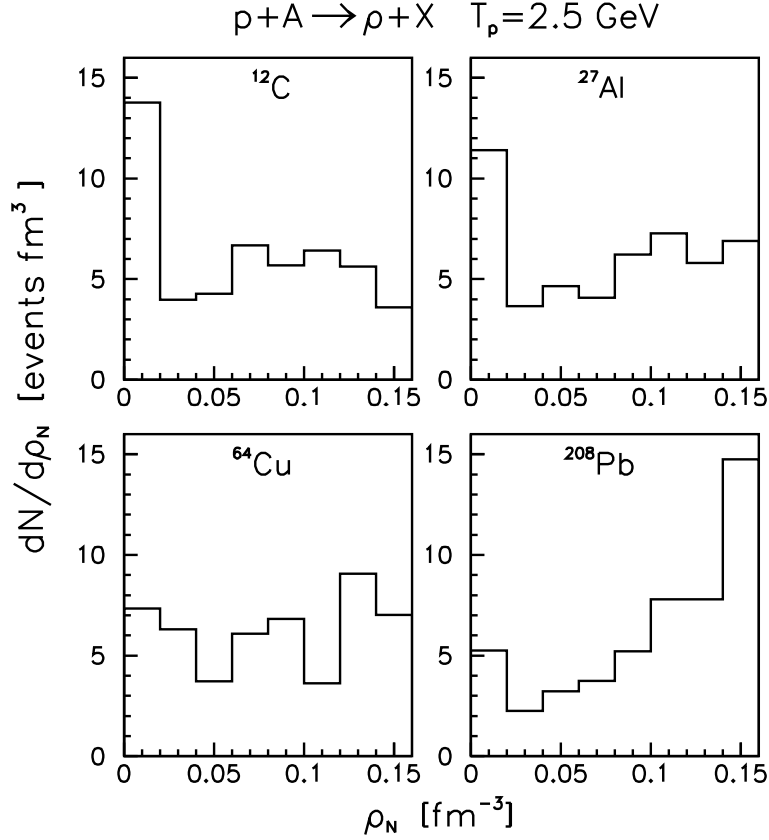


Figure 10: The ρ -meson decay rate as a function of the nuclear density for different targets at a bombarding energy of 2.5 GeV.

one should keep in mind that the cross section for ρ -meson production at low energies is substantially smaller.

Fig.10, furthermore, shows the ρ -decay rate as a function of the nucleon density at 2.5 GeV for the targets ^{12}C , ^{27}Al , ^{64}Cu and ^{208}Pb . While for the Pb -target a major fraction of ρ -mesons decays at normal nuclear matter density, this fraction decreases with the target mass significantly. However, even for ^{12}C still 50% of the ρ 's decay at densities $0.5\rho_0$ - ρ_0 such that modifications of the ρ -spectral function in the medium can still be tested with ^{12}C .

5.2 Calculations with a bare ρ spectral function

In actual experiments the invariant mass distribution of pion pairs from ρ -decay as presented in Fig. 8 is swamped by the background from pion pairs that stem from the reactions $pN \rightarrow \Delta\Delta \rightarrow 2\pi NN$ and $pN \rightarrow RN \rightarrow 2\pi NN$, where R is an intermediate resonance that decays into the two pion channel (cf. Fig.7a). The actual invariant mass distribution of pion pairs to be expected experimentally (within the cuts $p_z \leq 2 \text{ GeV}/c$ and $p_T \leq 0.8 \text{ GeV}/c$) is shown in Fig.11a) for $p + ^{12}\text{C}$ at 2.5 GeV when neglecting any medium modifications of the ρ -meson. The solid histogram in Fig.11a represents

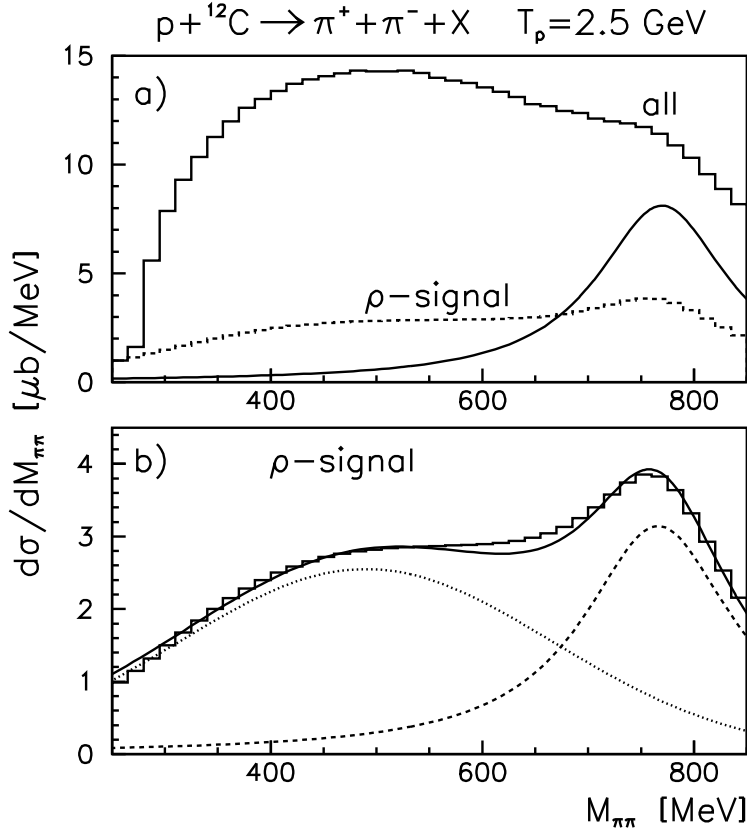


Figure 11: The invariant mass distribution of two pions from $p + {}^{12}\text{C}$ collisions at 2.5 GeV using the bare spectral function of the ρ -meson for $p_z \leq 2 \text{ GeV}/c$ and $p_T \leq 0.8 \text{ GeV}/c$. In a) the solid histogram shows the total $\pi - \pi$ invariant mass spectrum while the dashed histogram indicates the ρ signal after subtraction of the combinatorial background. The solid line is a Breit-Wigner distribution with the bare ρ -meson properties normalized to the total ρ -production cross section from the transport approach as expected in case of no final state interactions. In b) the histogram shows the ρ -meson signal from a) while the dotted line is the statistical spectrum; the dashed line is a Breit-Wigner function with the ρ -meson properties $M_0 = 766.9 \text{ MeV}$ and $\Gamma_0 = 173 \text{ MeV}$ and the solid line shows the sum as discussed in the text.

the pion pair mass distribution including the background pions as well as those from ρ -decay while the solid curve indicates the contribution from ρ -decay as obtained from the total ρ production cross section without any final state interactions. The latter solid line thus would represent a maximum ρ signal if all ρ -mesons would propagate out of the nucleus and decay in vacuum which, of course, is unrealistic.

In order to subtract the background from uncorrelated pion pairs we adopt a combinatorial method, i.e. mix pions from different events. This procedure was demonstrated in a recent experimental study of $\Delta(1232)$ -resonance excitation in heavy-ion collisions by Badala et al. [46] to be very effective for the extraction of a true correlation signal.

The dashed histogram in Fig.11a) shows the difference between the real and mixed invariant mass spectra and corresponds to pion pairs from ρ -decays including all final state interactions of the ρ -meson as well as its decay pions (cf. Fig. 8a). As discussed above the deviation of the solid line in Fig. 11a) from the dashed histogram is only due to ρ and pion final state interactions. Consequently, the ρ spectral function appears substantially distorted by conventional hadronic interactions.

According to Figs.9,10 a sizeable fraction of the ρ -mesons decays at very low nuclear density for ^{12}C or in the vacuum where its spectral function is well known. We thus can describe this 'outside' component approximately by a Breit-Wigner function

$$\frac{d\sigma}{dM_{\pi\pi}} = \frac{C_0}{(M_{\pi\pi} - M_0)^2 + \Gamma_0^2/4}, \quad (21)$$

where C_0 is some constant which (in absence of ρ -meson melting) is related to the total cross section of ρ -production from $p + ^{12}\text{C}$ collisions while M_0 and Γ_0 are the mass and width of the bare ρ -meson, respectively.

The π - π mass distribution, that is associated to the ρ -meson production from $p + ^{12}\text{C}$ collisions (after background subtraction), is shown again in Fig.11b) by the solid histogram. Apart from the 'outside' decay contribution a further fraction of ρ 's decays 'inside' the medium at nonzero density. Tentatively, we analyze this 'inside' component (together with all effects from final state interactions) in terms of a 'thermodynamical approach'. In this limit one can describe this part within the statistical model similar to the formalism developed in [47, 48] by

$$\frac{d\sigma}{dM_{\pi\pi}} = N \exp\left(-\frac{[M_{\pi\pi} - E_0]^2}{T_0^2}\right), \quad (22)$$

where the normalization N , average excitation energy E_0 and dispersion T_0 can be fitted to the ρ -mass spectrum for lower invariant mass $M_{\pi\pi}$ as shown in Fig.11b) by the dotted line. Accordingly, the solid line in Fig.11b) shows our fit to the ρ -meson signal by the sum of the Breit-Wigner function and statistical spectrum (22), where the first one involves the parameters $M_0=766.9$ MeV and $\Gamma_0=173$ MeV and is shown by the dashed line in Fig.11b).

So far, we have still discussed the results calculated with the bare ρ -meson properties. The final state interactions of ρ -mesons and pions from the $\rho \rightarrow \pi\pi$ decay yield an invariant mass distribution which is close to the recent predictions from Klingl and Weise [35] as discussed in Section 4 (cf. also Fig. 4). Any additional in-medium effects thus should show up in a further distortion of the invariant mass distribution.

5.3 In-medium modifications

As discussed above the QCD sum-rule approach by Hatsuda and Lee [2] predicts a shift of the ρ -mass with density according to Eq. (15) which corresponds to a shift of the ρ -meson pole. In order to explore if such an effect could be seen in the two pion decay mode we have performed calculations for $p + ^{12}\text{C}$ at 2.5 GeV employing Eq. (15). The solid histogram in Fig.12a) shows the total distribution in the invariant mass of two pions while the dotted histogram indicates the background obtained by mixing of pions

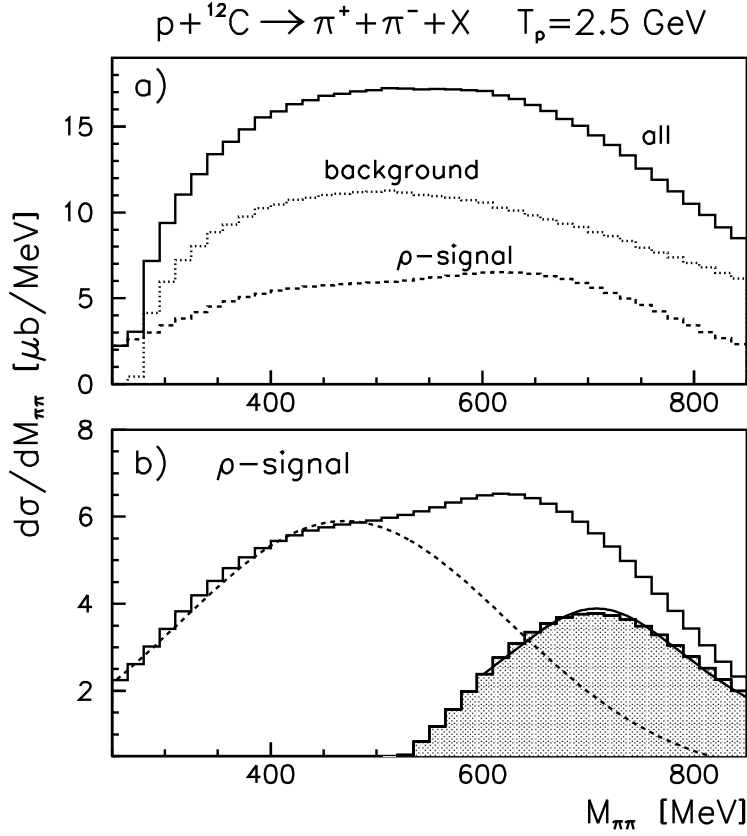


Figure 12: The invariant mass distribution of two pions from $p + {}^{12}\text{C}$ at 2.5 GeV employing the in-medium modification of the ρ -meson according to Hatsuda and Lee [2] for $\alpha = 0.16$. In a) the solid histogram shows the total $\pi-\pi$ invariant mass spectrum; the dotted histogram displays the background from uncorrelated pion pairs while the dashed histogram gives the ρ -mass distribution after subtraction of the background. In b) the solid histogram shows again the ρ -meson signal from a); the dashed line is a fit with Eq.(22) while the hatched histogram is the difference between the ρ signal and the fit Eq.(22), which can be described again by a Breit-Wigner function (solid line).

from different events. The latter is practically the same as that for those calculations performed with the bare ρ -meson properties (cf. section 5.2). The dashed histogram in Fig.12a) represents the ρ -signal as obtained by background subtraction. It is seen that not only the shape of the mass spectra, but also the absolute normalization are different from the calculations with the bare ρ -properties. The ρ -meson signal is shown again in Fig.12b) in terms of the solid histogram, which at first glance is quite complicated to analyze in order to extract in-medium properties of the ρ -meson.

We proceed as in section 5.2 and fit the spectrum with the function (22) as shown in Fig.12b) by the dashed line. The hatched histogram in Fig.12b) then shows the difference between the ρ -mass spectrum and distribution (22); it can again be fitted by a Breit-Wigner distribution (21) with $M = 708 \text{ MeV}$ and $\Gamma = 270 \text{ MeV}$. In comparison

with Fig.11b) the dropping of the ρ -meson mass thus appears possible to be extracted from the invariant mass distribution of two pions at least for light nuclei as ^{12}C .

We have also studied the modification of the ρ spectral function following the model from Klingl and Weise [35, 40]. For simplicity of the analysis we have 'switched-off' the final state interactions of pions stemming from ρ -decay in order to distinguish the change of the spectral function due to such processes from the in-medium modification (15). Fig.13 shows our results calculated for $p + ^{12}\text{C}$ collisions at 2.5 GeV. The hatched histogram stems from ρ -mesons, which decay outside or at the periphery of the nuclear target, while the solid histogram illustrates the pion pairs from the 'inside' decay of the ρ -mesons. Note that now the internal component has no pronounced resonance structure anymore and is similar to the spectrum from pion rescattering. The dashed histogram in Fig.13 shows the sum of these two components and the solid line is a fit (21) with the parameters $M = 765$ MeV and $\Gamma = 240$ MeV. The 'extracted' mass of the ρ -meson in this case is close to the bare mass while the width is considerably larger.

6 Summary

Within the coupled channel transport approach we have studied the production of ρ -mesons in proton-nucleus collisions and the detection of ρ -mesons via the pion decay mode ($\rho \rightarrow \pi + \pi$) employing different spectral functions for the in-medium ρ -mesons.

The elementary cross sections for ρ -production from $p + N$ and $\pi + N$ interactions as well as total and elastic $\rho + N$ final state interactions were calculated within the resonance model at low invariant energies and in quark-string models at higher invariant energies, which provided consistent results in a reasonable agreement with available experimental data. Note, however, that we have discarded interference effects in the resonance model and that more elaborate approaches will be necessary in future to pin down these cross sections more accurately.

Special attention was paid to the background from the production of two uncorrelated pions as well as for the attenuation of the ρ -meson yield due to ρN interactions as well as the final state interactions ($\pi + N$) of pions emerging from ρ -decay. We found that only light nuclear targets might be suitable for the experimental study of ρ -production via the pion decay mode. Appropriate kinematical cuts and background subtractions in principle allow to reconstruct the mass and width of the ρ -meson. However, for such a study a good mass resolution for the pion 4-momenta is required as well as a large detector acceptance.

We have investigated different schemes for the modification of the ρ -meson in nuclear matter and its consequences for the invariant mass distribution of two pions that can be detected asymptotically. The $\pi - \pi$ invariant mass spectra calculated within the hadronic scenario of Klingl and Weise [35, 36] are substantially different from those obtained by simulations based on the QCD sum-rule approach by Hatsuda and Lee [2]. These differences are much larger than the theoretical uncertainties arising from the local density approximation in the transport approach and might actually be studied experimentally by large area pion spectrometers e.g. at COSY, CELSIUS or the SIS. However, according to the authors opinion the actual shape of the ρ -meson spectral

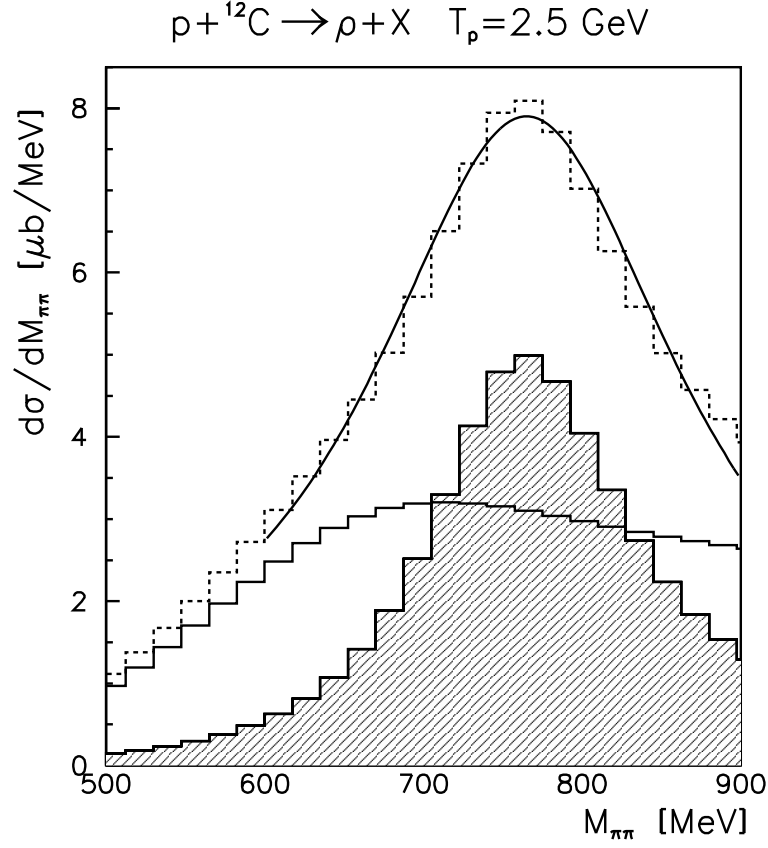


Figure 13: The invariant mass distribution of pion pairs from $p + {}^{12}\text{C}$ at 2.5 GeV including the in-medium modification of the ρ -meson according to Klingl and Weise [35, 40]. The hatched histogram shows the spectrum from ρ -mesons decaying 'outside' the nucleus, the solid histogram is the 'inside' component, while the dashed histogram is the sum of both. The solid line shows a Breit-Wigner fit with $M = 765 \text{ MeV}$ and $\Gamma = 240 \text{ MeV}$.

function cannot be determined accurately enough from the data analysis.

The authors gratefully acknowledge stimulating discussions with B. Friman, C.M. Ko, S. Leupold, U. Mosel and K. Tsushima. Furthermore, they like to thank F. Klingl, W. Weise, K. Saito, K. Tsushima and A.W. Thomas for providing their numerical results.

References

- [1] G. Brown and M. Rho, Phys. Rev. Lett. 66 (1991) 2720.
- [2] T. Hatsuda and S. Lee, Phys. Rev. C 46 (1992) R34.
- [3] G. Agakichiev et al., Phys. Rev. Lett. 75 (1995) 1272.
- [4] M. A. Mazzoni, Nucl. Phys. A 566 (1994) 95c; M. Masera, Nucl. Phys. A 590 (1995) 93c.
- [5] G. Q. Li, C. M. Ko, and G. E. Brown, Phys. Rev. Lett. 75 (1995) 4007.
- [6] W. Cassing, W. Ehehalt, and C. M. Ko, Phys. Lett. B 363 (1995) 35.
- [7] W. Cassing, W. Ehehalt, and I. Kralik, Phys. Lett. B 377 (1996) 5.
- [8] E. L. Bratkovskaya and W. Cassing, Nucl. Phys. A 619 (1997) 413.
- [9] A. Drees, Nucl. Phys. A 610 (1996) 536c.
- [10] W. Schön, H. Bokemeyer, W. Koenig and V. Metag, Acta Physica Polonica B 27 (1996) 2959.
- [11] W. Cassing, Ye.S. Golubeva, A.S. Iljinov, and L.A. Kondratyuk, Phys. Lett. B 396 (1997) 26.
- [12] A. Sibirtsev, W. Cassing and U. Mosel, Z. Phys. A 358 (1997) 357.
- [13] B. Nilsson-Almqvist and E. Stenlund, Comp. Phys. Comm. 43 (1987) 387.
- [14] S. Teis, W. Cassing, M. Effenberger, A. Hombach, U. Mosel, and Gy. Wolf, Z. Phys. A 356 (1997) 421.
- [15] B.A. Li and C.M. Ko, Phys. Rev. C 52 (1995) 2037.
- [16] G.E. Brown, C.M. Ko, Z.G. Wu and L.H. Xia, Phys. Rev. C 43 (1991) 1881.
- [17] M. Effenberger, A. Hombach, S. Teis and U. Mosel, Nucl. Phys. A 613 (1997) 353 ; A 614 (1997) 501.
- [18] Landolt-Börnstein, New Series, ed. H. Schopper, I/12 (1988)

- [19] A. Sibirtsev, Nucl. Phys. A 604 (1996) 455.
- [20] Particle Data Group, Phys.Rev. D 50 (1994) 1173.
- [21] B. Friman, private communication
- [22] H. Joos and G. Kramer, Z. Phys. 178 (1964) 542.
- [23] B. Friman and M. Soyeur, Nucl. Phys. A 600 (1996) 477.
- [24] R. Machleidt, Adv. Nucl. Phys. 19 (1989) 189.
- [25] R. Anderson et al., Phys. Rev. D 1 (1970) 27.
- [26] R.M. Egloff et al., Phys. Rev. Lett. 43 (1979) 657.
- [27] J. Ballam et al., Phys. Rev. D 7 (1973) 3150.
- [28] R.L. Anderson et al., Phys. Rev. D 4 (1971) 3245.
- [29] P. Danielewicz and G.F. Bertsch, Nucl. Phys. A 533 (1991) 712.
- [30] T. Hatsuda, nucl-th/9702002 (1997).
- [31] K. Saito, K. Tsushima and A.W. Thomas, nucl-th/9703011 (1997).
- [32] K. Tsushima, private communication.
- [33] T. Hatsuda, S.H. Lee and H. Shiomi, Phys. Rev. C 52 (1995) 3364.
- [34] X. Jin and D.B. Leinweber, Phys. Rev. C 52 (1995) 3344.
- [35] F. Klingl and W. Weise, Nucl. Phys. A 606 (1996) 329.
- [36] F. Klingl and W. Weise, nucl-th/97022240 (1997).
- [37] R. Rapp, G. Chanfray and J. Wambach, Nucl. Phys. A 617 (1997) 472.
- [38] G. Chanfray, R. Rapp and J. Wambach, Phys. Rev. Lett 76 (1996) 368.
- [39] B. Friman and H.J. Pirner, Nucl. Phys. A 617 (1997) 495.
- [40] F. Klingl, private communication.
- [41] W. Ehehalt and W. Cassing, Nucl. Phys. A 602 (1996) 449.
- [42] W. Cassing, E.L. Bratkovskaya, U. Mosel, S. Teis, and A. Sibirtsev, Nucl. Phys. A 614 (1997) 415; E.L. Bratkovskaya, W. Cassing, and U. Mosel, Nucl. Phys. A 622 (1997) 593.
- [43] J. Papp et al., Phys. Rev. Lett. 34 (1975) 601.
- [44] A. Schmidt and R. Blankenbecler, Phys. Rev. D 15 (1977) 3321.

- [45] M. Debowski et al., Z. Phys. A 356 (1996) 313.
- [46] A. Badala, R. Barbera, A. Bonasera, A. Palmeri, G.S. Pappalardo, F. Riggi, A.C. Russo, G. Russo, R. Turrisi, Phys. Rev. C 54 (1996) R2138.
- [47] C. Gale and J. Kapusta, Phys. Rev. C 35 (1987) 2107.
- [48] P. Koch, Z. Phys. C 57 (1993) 283.